

From G-quartets to G-ribbon gel by concentration and sonication control†

Cite this: *Org. Biomol. Chem.*, 2013, **11**, 1525

Luyan Meng, Keyin Liu, Shuli Mo, Yueyuan Mao and Tao Yi*

Two guanosine analogues have been designed and synthesized by connecting one (1) or three adamantane branches (2). The compound containing a single adamantane branch formed G-quartets in acetonitrile solution, and was then transformed into a G-ribbon gel at concentrations higher than the critical gelation concentration. In contrast, the compound with three adamantane branches precipitated after a heating-cooling process. By means of circular dichroism and UV/visible spectra, NMR, SEM, and structural studies, the mechanism of the formation of the G-quartets and G-ribbon gel, as well as the difference in the self-assembly modes of the two compounds, have been fully elucidated. Compound 1 firstly self-assembled into G-quartets in solutions in the concentration range 5.0×10^{-4} to 1.0×10^{-2} M, and these G-quartets were transformed into a G-ribbon on further increasing the concentration. Gelation occurred when the G-ribbon self-assembled into a hexagonal columnar structure with the help of intermolecular hydrogen-bonding and hydrophobic interactions. This gel was sensitive to sonication and underwent a morphology change from a columnar structure to a flower-like structure composed of flakes. In contrast, due to steric hindrance, compound 2 only assembled into a spherical structure based on hydrophobic interactions.

Received 13th November 2012,
Accepted 10th January 2013

DOI: 10.1039/c3ob27204d

www.rsc.org/obc

Introduction

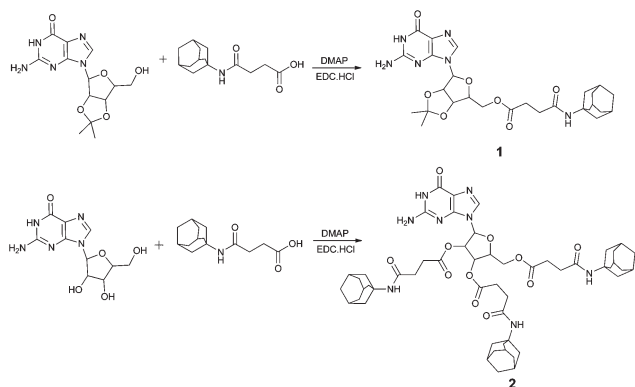
Supramolecular self-assembly through non-covalent interactions, including hydrogen-bonding, π - π stacking, hydrophilic and hydrophobic interactions, electrostatic interactions, and van der Waals forces, offers potential applications in biology and nanotechnology.¹ DNA nucleobases carry the key information of inheritance by utilizing a variety of cooperative and non-covalent interactions.¹ Among nucleobases, guanine is of particular interest. Due to the abundant proton donor and acceptor sites, which are fundamental in self-recognition and self-assembly processes, guanosine can self-assemble into dimeric,² G-quartet,³ ribbon-like,⁴ and helical structures⁵ under certain circumstances, which makes it a promising moiety for designing functional materials.⁶ In particular, G-quartets have attracted considerable attention over the past two decades because of their additional biological significance.⁷ For example, DNA sequences with guanine-repeated G-quadruplex secondary structures have been considered as novel targets for anticancer drug therapy.^{8,9}

Guanosine analogues usually self-assemble into hydrogen-bonded dimers or ribbons in the absence of an appropriate

template cation, except in a few special cases. Sessler *et al.* attached a dimethylaniline moiety to the C8 position of guanosine and obtained a G-quartet in the absence of alkali metal cations, which showed how synthetic chemistry could be used to produce unnatural nucleobases for the non-covalent synthesis of stable supramolecular assemblies.¹⁰ Besenbacher *et al.* showed that guanine was able to form an “empty” G-quartet network on a gold surface, a process that was kinetically rather than thermodynamically controlled.¹¹ Highly ordered supramolecular motifs formed by guanosine derivatives may be reversibly interconverted, as exemplified by the transformation between G-quartet-based architectures and hydrogen-bonded G-ribbons with the help of an exterior synergistic effect of potassium ions, [2.2.2]cryptand, and trifluoromethanesulfonic acid.¹² Meanwhile, DNA G-quadruplexes have been proposed to play an important role in the maintenance of telomere length as they cannot be extended by telomerase. Mashimo *et al.* demonstrated that hairpin and triplex structures were energetically feasible intermediates along the telomeric DNA G-quadruplex folding pathway.¹³ Therefore, exploration of the conversion between G-quartets and other self-assembled forms of guanosine is very useful for obtaining a better understanding of the formation and stability of DNA G-quadruplexes.

Amphiphilic compounds have received much attention over the past few decades because of their particular structural characteristics and importance in biological research.¹⁴ Some

Department of Chemistry, Fudan University, 220 Handan Road, Shanghai 200433, China. E-mail: yitao@fudan.edu.cn; Fax: +86-21-55664621; Tel: +86-21-55664330
†Electronic supplementary information (ESI) available: Details of supplementary spectra and images. See DOI: 10.1039/c3ob27204d



Scheme 1 Chemical structure and synthetic route of **1** and **2**.

amphiphilic molecules can form vesicles, tubes, or even gel networks.¹⁵ Low-molecular-weight organogels (LMOGs) are especially interesting due to their potential applications in materials, sensors, drug delivery, and so on.¹⁶ Amphiphilic guanosine derivatives obtained by modification of glycosyl with a hydrophobic group not only possess the intrinsic properties of guanine itself, but also an additional hydrophobic interaction, which may be exploited to manipulate molecular self-assembly behavior by adjusting the micro-environment, such as concentration, solvent, *etc.* In this work, we have designed and synthesized two amphiphilic guanosine derivatives by modifying the glycosyl group of guanosine with an adamantane moiety (**1** and **2** in Scheme 1). Surprisingly, we found that **1** could form G-quadruplexes at low concentrations in acetonitrile solution without templating ions, and these G-quadruplexes were transformed into a gel network on increasing the concentration. The driving force and the mechanism of this structural transformation by molecular self-assembly have been studied in depth.

Experiment

General

All of the starting materials were obtained from commercial suppliers and used as received. Moisture sensitive reactions were performed under an atmosphere of dry argon. Amantadine hydrochloride (99%) was provided by Alfa Aesar, and other chemicals were supplied from Sinopharm Chemical Reagent Co., Ltd (Shanghai). Column chromatography was carried out on silica gel (200–300 mesh). The ¹H NMR (400 MHz) and ¹³C NMR (100 MHz) spectra were recorded on a Mercury plus-Varian instrument. Proton chemical shifts are reported in parts per million downfield from tetramethylsilane (TMS). HR-MS was recorded on an LTQ-Orbitrap mass spectrometer (Thermo Fisher, San Jose, CA). Melting points were determined on a hot-plate melting point apparatus XT4-100A without correction.

Synthesis of **1** and **2**

The synthesis of **1** and **2** is shown in Scheme 1. 2',3'-Isopropylidene guanosine and (*N*-adamantylcarbamoyl) propionic acid were synthesized according to the previous reports¹⁷ and characterized by ¹H NMR (see details in ESI†).

Synthesis of 1. A mixture of 2',3'-isopropylidene guanosine (0.32 g, 1.0 mmol), (*N*-adamantylcarbamoyl)propionic acid (0.30 g, 1.2 mmol), DMAP (0.12 g, 1.0 mmol) and EDC HCl (0.80 g, 4.0 mmol) in dry DMF (10 mL) was stirred overnight at room temperature under an argon atmosphere. The solvent was removed using a rotary evaporator equipped with high vacuum. The residue was dissolved in CH₂Cl₂ (100 mL), washed with water (50 × 3 mL). The organic layer was collected and evaporated to dryness; the crude product was purified by column chromatography [SiO₂, CH₂Cl₂-MeOH (10 : 1, v/v)] to give a white solid (yield 90%). Mp: 251–253 °C. ¹H NMR (400 MHz, DMSO-d₆, 298 K): δ 10.69 (s, 1H), 7.87 (s, 1H), 7.32 (s, 1H), 6.53 (s, 2H), 6.00 (d, *J* = 2.1 Hz, 1H), 5.22 (dd, *J* = 6.3, 2.1 Hz, 1H), 5.15–5.07 (m, 1H), 4.30–4.19 (m, 2H), 4.19–4.09 (m, 1H), 2.42 (d, *J* = 7.2 Hz, 2H), 2.30 (d, *J* = 7.0 Hz, 2H), 1.97 (s, 3H), 1.88 (s, 6H), 1.59 (s, 6H), 1.51 (s, 3H), 1.32 (s, 3H). ¹³C NMR (100 MHz, DMSO-d₆, 298 K): δ 172.37, 170.01, 156.90, 153.80, 150.61, 136.26, 116.97, 113.37, 88.42, 84.48, 83.86, 81.09, 64.03, 50.67, 41.04, 36.10, 30.59, 29.09, 28.90, 27.04, 25.31. HRMS (ESI, *m/z*): calcd for C₂₇H₃₆N₆O₇ [M + H]⁺, 557.2724; found: 557.2730.

Synthesis of 2. **2** was prepared with the same method for **1** using guanosine (0.09 g, 0.32 mmol) instead of 2',3'-isopropylidene guanosine (0.40 g, 1.0 mmol). Mp: 198–200 °C. ¹H NMR (400 MHz, DMSO-d₆, 298 K) δ 10.73 (s, 1H), 7.92 (s, 1H), 7.34 (d, *J* = 26.8 Hz, 3H), 6.55 (s, 2H), 5.98 (d, *J* = 5.6 Hz, 1H), 5.84–5.65 (m, 1H), 5.49 (s, 1H), 4.31 (dd, *J* = 42.8, 9.8 Hz, 3H), 2.54 (d, *J* = 6.3 Hz, 2H), 2.40–2.20 (m, 6H), 2.08–1.74 (m, 27H), 1.59 (s, 18H). ¹³C NMR (100 MHz, DMSO-d₆, 298 K) δ 172.28, 171.65, 171.52, 169.88, 169.77, 169.60, 156.81, 153.98, 151.21, 135.75, 130.72, 128.82, 116.94, 84.76, 79.72, 72.27, 70.35, 63.33, 50.71, 50.67, 41.05, 36.14, 30.54, 30.42, 28.94, 28.78. HRMS (ESI, *m/z*): calcd for C₅₂H₇₀N₈O₁₁ [M + H]⁺, 983.5242; found: 983.5223.

Gelation test for organic fluids

The gelator and solvent were put in a septum-capped test tube and heated (>80 °C) until the solid was dissolved. The sample vial was then cooled to 25 °C (room temperature). Qualitatively, gelation was considered successful if no sample flow was observed upon inversion of the container at room temperature (the inverse flow method).

Techniques

FTIR spectra were recorded by using an IRPRESTIGE-21 spectrometer (Shimadzu). SEM images were obtained using an FE-SEM S-4800 (Hitachi) instrument. Samples were prepared by spinning the samples on glass slices and coating with Au. The samples were prepared by coating the diluted wet gels on a copper grid at room temperature and freeze drying (EYELA,

FDU-1200) for 24 h. Powder X-ray diffractions were generated by using a Philips PW3830 sealed-tube X-ray generator (Cu target, $\lambda = 0.1542$ nm) with a power of 40 kV and 50 mA. CD (circular dichroism) spectra and UV-Vis absorption spectra were recorded on a MOS-450 spectropolarimeter and a UV-vis 2550 spectroscope (Shimadzu), respectively.

Calculation of the equilibrium constant K for the G-quartet

The equilibrium for the formation of G-quartet structure was shown by eqn (1) and the equilibrium constant, K , was given by eqn (2):¹⁸



$$K = [G_4]/[G]^4 = [G_4]/(c_0 - 4[G_4])^4 \quad (2)$$

where c_0 represents the total concentration of initial **1**. As we know, the CD ellipticity (θ) meets eqn (3):

$$\theta = 2.303(A_L - A_R)/4 = 0.576\Delta\epsilon cl \quad (3)$$

where $\Delta\epsilon$, c and l represent the difference values of molar extinction coefficients for left and right circularly polarized light, the molar concentration of an optically active molecule and the path length, respectively. Thus eqn (3) can be simplified into (4). The equilibrium constant K for the G-quartet can be obtained by eqn (5):

$$[G_4] = k\theta \quad (4)$$

$$K = k\theta/(c_0 - 4k\theta) \quad (5)$$

where k represents the coefficient.

Results and discussion

The solubility and gelation properties of **1** and **2** are summarized in Table 1. To our knowledge, lipophilic guanosine derivatives are often present in the form of monomeric species in aprotic solvents, especially in dimethylsulfoxide,¹⁹ but are likely to form G-ribbon structures in the absence of a cationic

template in chlorinated organic solvents.⁴ Protic solvents, such as ethanol and methanol, are not conducive to molecular self-assembly of lipophilic guanosine derivatives because of their competing hydrogen bonding. As we expected, **1** and **2** were found to dissolve freely in many polar solvents, including chloroform, ethanol, methanol, tetrahydrofuran, dimethylformamide, dimethylsulfoxide and dioxane, whereas they proved to be insoluble in hexane and precipitated from ethyl acetate. However, **1** formed a transparent gel and an opaque gel after a heating-cooling process with critical gelation concentrations (CGCs) of 5 mg mL⁻¹ and 25 mg mL⁻¹ in dichloromethane and acetonitrile, respectively. Moreover, ultrasound had an influence on the gel formation of **1**. Sonication reduced its CGC to 20 mg mL⁻¹ in acetonitrile, and promoted the gelling of **1** in chloroform, with a CGC of 25 mg mL⁻¹. It is obvious that the balance between hydrophobicity and hydrophilicity, as well as the steric effect react on the gelation properties of these compounds. The three adamantane moieties in compound **2** increase the hydrophobic property and the steric effect, thus reduce its gelation capability. Compound **2** was found to be soluble in hot acetonitrile (above 100 °C), but gradually precipitated after cooling to room temperature. Hence, the self-assembly behavior of the two compounds in acetonitrile was studied in more detail.

At the present time, the outstanding sensitivity of circular dichroism (CD) makes it the main tool for studying biological macromolecular chirality and perturbations by external factors.²⁰ In order to gain information on the structure and mechanism of gel formation, a large range of concentrations of **1** in CH₃CN from solution (1.0 × 10⁻⁴ M) to stable gel state (0.1 M) were investigated by CD spectroscopy, and the spectra are shown in Fig. 1. For guanosine derivatives, if the tetramers of the G-quartet-based assemblies were rotated with respect to one another, a double-signed CD signal would be expected in the region 230–330 nm, characteristic of the π - π^* transitions of the guanosine chromophore. It is evident from Fig. 1a that the CD signal of **1** at a concentration lower than 2.5 × 10⁻⁴ M was very weak. When the concentration was increased to 5.0 × 10⁻⁴ M, two opposite signed bands at 263 and 293 nm appeared, the intensity of which increased with increasing concentration up to 5.0 × 10⁻² M (Fig. 1a and 1b). According to a previous report, the presence of opposite signed bands at ca. 290 and 260 nm is diagnostic of heteropolar stacking.²¹ The CD spectra of **1** strongly suggest a G-quartet conformation with heteropolar stacking having D_4 symmetry. The equilibrium constant of G-quartet formation was calculated from the CD spectral change in the concentration range 5.0 × 10⁻⁴ to 3.0 × 10⁻³ M (see details in the experiment part). The influence of concentration on the CD ellipticity at 263 nm is illustrated in the inset in Fig. 1a. The equilibrium constant K for G-quartet formation was estimated to be 6.3626 × 10⁹ M⁻³ from a linear fitting with a coefficient of $k = 4.7455 \times 10^{-6}$ ($R^2 = 0.9956$).

With a further increase in concentration from 1.0 × 10⁻² to 5.0 × 10⁻² M (gel formation), the band located at 263 nm gradually shifted to longer wavelengths and diminished in

Table 1 Gelation properties of **1** and **2**^a

Solvent	1	2
CH ₃ CN	G (25) ^b , G (20) ^c	P
CH ₂ Cl ₂	G (5) ^b	S
CHCl ₃	S ^b , G (25) ^c	S
MeOH	S	S
EtOH	S	S
EtOAc	P	P
THF	S	S
DMSO	S	S
DMF	S	S
Hexane	I	I

^a G = gel; P = precipitation; S = solution; I = insoluble. The critical gelation concentrations of the gelators are given in the parentheses (mg mL⁻¹). ^b Heated to dissolve, then cooled to room temperature. ^c Heated to dissolve, then treated with ultrasound for 30 s, ultrasound power: 0.16 W cm⁻², 40 kHz.

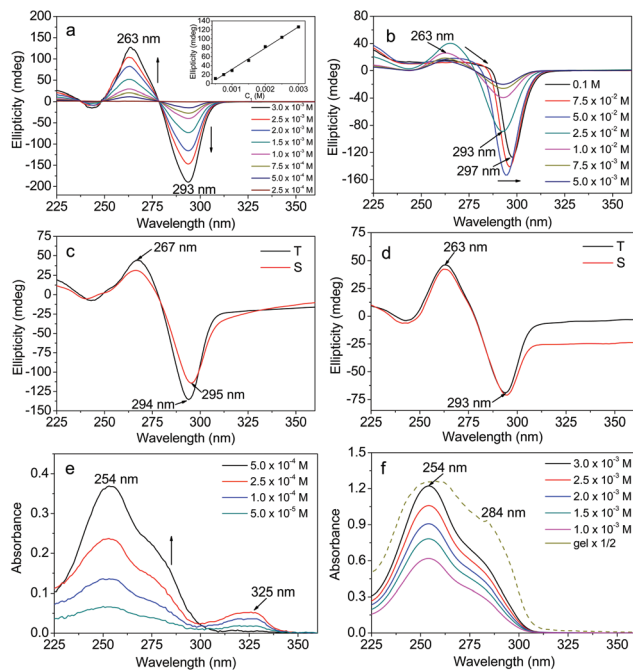


Fig. 1 CD spectra of **1** in CH_3CN under different concentrations: (a) 2.5×10^{-4} – 3.0×10^{-3} M (inset is the Job's plot for CD ellipticity at 263 nm in the concentration range of 5.0×10^{-4} – 3.0×10^{-3} M; cell length, 1.0 mm); (b) 5.0×10^{-3} – 0.1 M (cell length, 0.1 mm); CD spectra of **1** in CH_3CN with concentrations of (c) 3.6×10^{-2} M and (d) 1.0×10^{-2} M before (T) and after sonication (S); UV-visible absorption spectra of **1** in CH_3CN solution with different concentrations of (e) 5.0×10^{-5} – 5.0×10^{-4} M (cell length, 0.5 mm), and (f) 1.0×10^{-3} – 3.0×10^{-3} M and gel in CH_3CN (5.0×10^{-2} M) (cell length, 0.1 mm; absorbance of gel was divided by 2 for clear comparison).

intensity, while the opposite band located at 293 nm intensified with no wavelength change. Beyond 5.0×10^{-2} M, the single band located at 293 nm was gradually shifted to 297 nm and slightly diminished in intensity during the stable gel formation. According to previously reported results,²² a negative band of moderate intensity at around 300 nm supported the presence of stacked monomers or stacked dimers. In summary, **1** first self-assembled into a G-quartet at low concentration. The G-quartet dissociated with increasing concentration, and the molecules subsequently aggregated in the form of stacked monomers or stacked dimers upon gel formation.

The CD spectra of the sample (3.6×10^{-2} M, 20 mg mL^{-1}) before and after sonication were compared. The positions of the CD bands of the gel (S-gel) after sonication were slightly red shifted from 294 to 295 nm, but the intensity obviously decreased (Fig. 1c). This phenomenon is similar to the effect of increasing concentration. The decreased intensity of the S-gel compared to the sol with the same concentration can be ascribed to the increased accumulation after sonication. This may be the reason for the decrease of CGC by sonication. However, for the sample with the concentration lower than CGC of S-gel, sonication has almost no influence on the CD spectra (Fig. 1d).

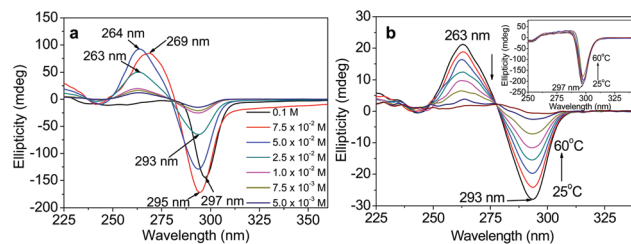


Fig. 2 (a) CD spectral changes of the gel formed by **1** in acetonitrile (0.1 M) upon addition of 0, 1/3, 1, 3, 9, 12.3 to 19 equivalent volumes of acetonitrile; (b) temperature variable CD spectra of G-quartets (2.5×10^{-3} M, cell length 0.5 mm) and gel (inset, 0.1 M, cell length 0.1 mm) of **1** in acetonitrile, temperature from 25 to 60 °C with an interval of 5 °C.

The corresponding UV/visible absorption spectra of **1** were also examined and showed two absorption bands at 254 and 325 nm at lower concentrations before the G-quartets were formed (5.0×10^{-4} M) (Fig. 1e), which could be ascribed to π - π^* and n - π^* transitions ($\text{C6}=\text{O}$) of the guanine chromophore, respectively. When the concentration was higher than 5.0×10^{-4} M, G-quartets were formed with $\text{C6}=\text{O}$ being involved in the intermolecular hydrogen bonds, so that the n - π^* transition of the guanine chromophore was weakened. As a result, the absorption band centered at 325 nm disappeared (Fig. 1f). In the gel formed at a concentration of 5.0×10^{-2} M, a red-shifted shoulder band at 284 nm was observed, indicating a π - π interaction between the chromophores. This conjecture was consistent with the experimental CD data.

To check the reversibility of the self-assembly process, the transformation from the gel network to G-quartets upon dilution of the self-assembled structure with acetonitrile was investigated by CD spectroscopy (Fig. 2a). When the gel was diluted from 0.1 M to 7.5×10^{-2} M in acetonitrile, two opposite signed bands at 269 and 295 nm appeared in place of the original negative band located at 297 nm. Upon further dilution of the gel to 2.5×10^{-2} M, the opposite signed bands were gradually blue-shifted to 263 and 293 nm, at which they remained upon further dilution with acetonitrile. Thus, the acetonitrile gel of **1** completely reverted to G-quartets upon dilution. Furthermore, to gain insight into the stability of the G-quartets and the gel, the temperature dependences of the CD spectra of the G-quartets (2.5×10^{-3} M) and the G-ribbon (gel state, 0.1 M) of **1** in acetonitrile were measured (Fig. 2b). The positions of the CD bands at 263 and 293 nm characteristic of G-quartets remained unchanged with increasing temperature, but they showed a sharp decrease in intensity and eventually disappeared at 60 °C. This indicated that the G-quartet structure was thermodynamically unstable, dissociating to the monomer at higher temperature. In contrast, the CD spectra of the G-ribbon structure in the gel state showed no obvious changes in either location or intensity when the temperature was increased from 25 to 60 °C, which indicated that the G-ribbon structure was comparatively stable within the studied temperature range (Fig. 2b, inset).

Moreover, the CD spectra of **1** in other solvents, such as tetrahydrofuran, chloroform, dimethylsulfoxide (DMSO), and

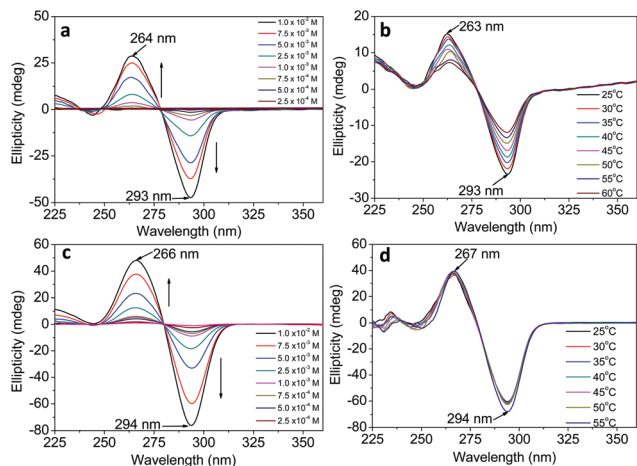


Fig. 3 CD spectra of **1** in (a) tetrahydrofuran and (c) chloroform in the concentration range of 2.5×10^{-4} – 1.0×10^{-2} M; temperature variation CD spectra of **1** in (b) tetrahydrofuran and (d) chloroform (2.5×10^{-3} M) (cell length, 0.5 mm).

methanol, at different concentrations were also measured. The CD spectra of **1** in tetrahydrofuran were similar to those in acetonitrile, with two opposite signed bands appearing at 263 and 293 nm, the intensity of which decreased with increasing temperature (Fig. 3a and 3b). In chloroform (Fig. 3c and 3d), although two opposite bands were seen at 266 and 294 nm, neither the positions nor the intensities of these two bands showed any obvious changes with increasing temperature, indicating that the G-quartet self-assembly of **1** in chloroform was more stable than that formed in acetonitrile. The G-quartet formed in chloroform could not be transformed into a gel by increasing the concentration. However, solutions of **1** in chloroform at concentrations higher than 25 mg mL^{-1} (4.5×10^{-2} M) could be gelled with the aid of sonication. No signal was detected in the CD spectrum of **1** in DMSO, indicating that the molecule remained predominantly in a monomeric form in this solvent (Fig. S1, ESI[†]). CD spectra recorded in methanol were similar to that in DMSO, except for some slight fluctuation at high concentrations, which may have been due to hydrogen-bonding competition between **1** and methanol (Fig. S2, ESI[†]).

The corresponding ^1H NMR spectra also proved the formation of G-quartets. The ^1H NMR spectral region between $\delta = 4$ and 13 ppm proved to be useful for characterizing the self-assembly of guanosine derivatives, especially the association of G-quartets. The ^1H NMR spectrum of **1** in DMSO- d_6 showed sharp and well-defined signals that were indicative of the predominant presence of monomeric species (Fig. S3, ESI[†]). In CD_3CN (Fig. 4), the singlet signal of the imino proton (H-N1) of **1** was downfield shifted from $\delta = 10.69$ ppm and split into three peaks in the region $\delta = 12.1$ – 12.3 ppm. This indicated G-quartet stacking involving both *anti* (located at lower field) and *syn* conformers.²³ The chemical shifts of these signals remained unchanged when the concentration of the solution was increased from 5.0×10^{-3} to 5.0×10^{-2} M, but the relative intensity of the signals attributable to the

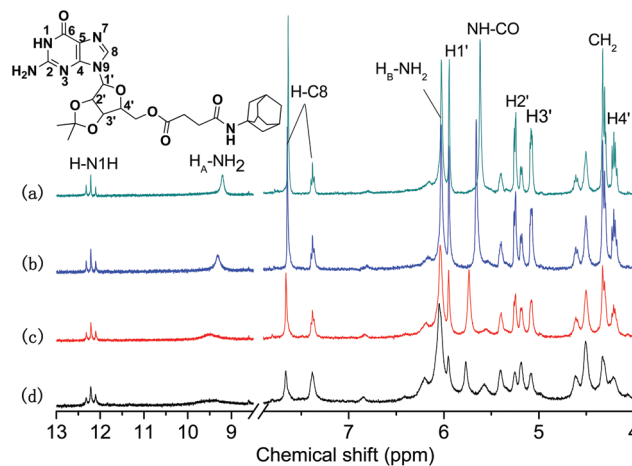


Fig. 4 ^1H NMR spectra of **1** with different concentrations (a) 5.0×10^{-3} M, (b) 1.0×10^{-2} M, (c) 2.5×10^{-2} M and (d) 5.0×10^{-2} M in CD_3CN .

anti-conformer decreased and all of the signals became broad. When the concentration was lower than 1.0×10^{-2} M, the typical signal of H-C8 was split into two bands, located at $\delta \approx 7.7$ and 7.4 ppm. The signal of H-C8 in the *syn* conformer was observed at $\delta \approx 7.4$ ppm, which is typical of structures formed by assembled G-quartets.²³ The signal of the $-\text{NH}_2$ protons originally located at $\delta = 6.5$ ppm in DMSO was split into two broad bands at $\delta = 9.3$ ppm ($\text{H}_A\text{-NH}_2$) and 6.0 ppm ($\text{H}_B\text{-NH}_2$) in the concentration range 5.0×10^{-3} to 1.0×10^{-2} M in CD_3CN . This splitting of the resonance of the $-\text{NH}_2$ protons was also indicative of G-quartet formation, with $\text{H}_A\text{-NH}_2$ being involved in H-bonding.²⁴ Other protons showed almost no change in chemical shifts but broadened with the increased concentration. Therefore, we could conclude that G-quartets were formed before the concentration reached 1.0×10^{-2} M. The broadening and the downfield shift of the signal of $\text{H}_A\text{-NH}_2$ with increasing concentration signified dissociation of the G-quartets and the formation of a G-ribbon structure. When the concentration reached 5.0×10^{-2} M, the NH proton signal of the amantadine group at $\delta = 5.62$ ppm split into two peaks at $\delta = 5.76$ and 5.57 ppm, which indicated that the amantadine amide group participated in the intermolecular H-bond self-assembly. In other words, two kinds of intermolecular interactions were involved in the aggregation of **1** in the gel state, the first being the assembly of two molecules of **1** into a G-ribbon building block through multiple intermolecular hydrogen bonds between guanine moieties, and the second being the further aggregation of the G-ribbons through intermolecular hydrogen bonding of amantadine amide groups with the cooperation of hydrophobic interactions.

The morphology and structure of the gel formed by **1** were investigated by scanning electron microscopy (SEM) and X-ray diffraction analysis (XRD). SEM images of the xerogel of **1** obtained after a heating-cooling process (T-xerogel) showed a hexagonal columnar structure with the width of the column in the range 4–9 μm (Fig. 5a and 5b). Meanwhile, SEM images of the S-xerogel of **1** obtained by sonication revealed a twisted

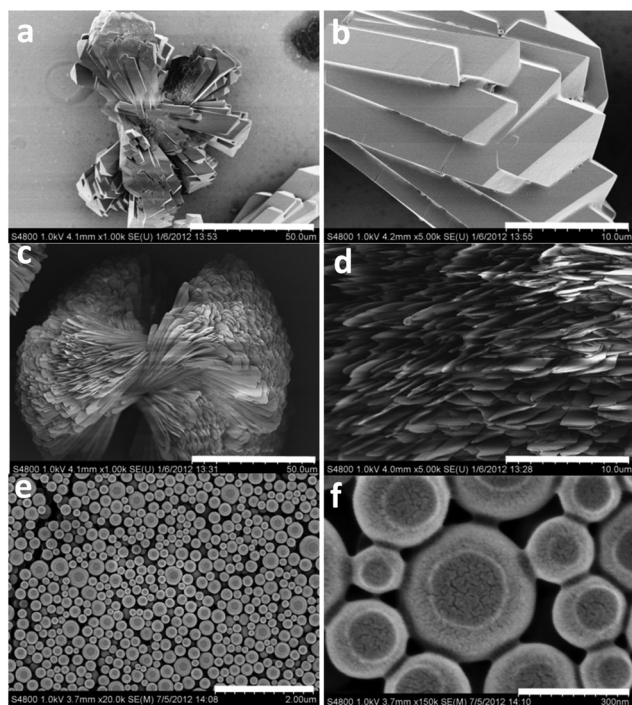


Fig. 5 SEM images of T-xerogel (a and b) and S-xerogel (c and d) of **1** in CH_3CN ; SEM images of precipitation of **2** in CH_3CN (e and f); scale bar: (a) 50 μm , (b) 10 μm , (c) 50 μm , (d) 10 μm , (e) 2 μm , (f) 300 nm.

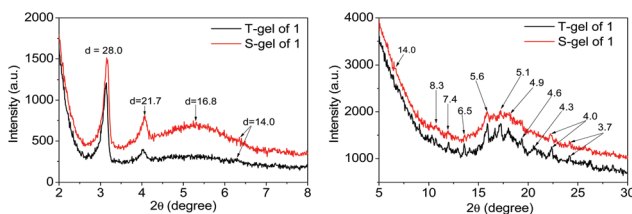


Fig. 6 Powder X-ray diffraction patterns of xerogel of **1** from CH_3CN at room temperature.

flower-like structure made up of numerous sheets, with the average width of each sheet being about 2 μm (Fig. 5c and 5d). However, the xerogels of **1** formed with or without sonication displayed similar X-ray diffraction profiles (Fig. 6). This indicated that the two kinds of gels were constructed from the same substructure. Small-angle X-ray scattering measurements showed a series of peaks corresponding to d -spacings of 28.5, 16.8, and 14.0 Å, with a ratio of $1 : 1/\sqrt{3} : 1/\sqrt{4}$, indicating the formation of a Col_h structure with a structure parameter of $a = 32.9$ Å, consistent with the result from the SEM images. Molecular modeling suggested that two molecules of **1** were assembled through intermolecular hydrogen bonds between guanine moieties at a spacing of approximately 32.7 Å (Fig. S7, ESI[†]), which is very close to the value of the parameter a (32.9 Å). Thus, we speculated that **1** self-assembled into a G-ribbon structure *via* dimer units and further aggregated into a hexagonal columnar structure in the gel state.

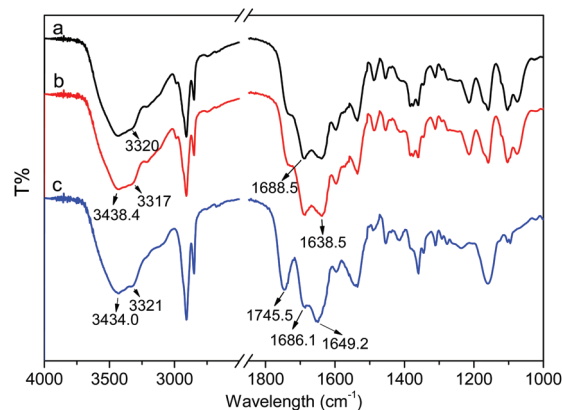


Fig. 7 IR spectra of xerogel of (a) T-gel, (b) S-gel of **1** and (c) precipitation of **2**.

In contrast, with three adamantane groups connected to the glycosyl group of guanosine, **2** precipitated from acetonitrile after a heating-cooling process. SEM images of the precipitate revealed globular structures of differing diameters in the range 100–300 nm (Fig. 5e and 5f). Transmission electron microscopy (TEM) revealed that these globular structures were solid (Fig. S4, ESI[†]). The XRD profile of the precipitate of **2** showed a peak at 23.4 Å (Fig. S5, ESI[†]), close to the length of the molecule of **2** (Fig. S6, ESI[†]). Evidently, the significant steric effect caused by the three adamantane branches greatly weakened the intermolecular hydrogen-bonding interaction between the guanine moieties of **2**. Therefore, **2** shows better solubility in most polar solvents.

The difference in the intermolecular hydrogen-bonding patterns seen in **1** and **2** was corroborated by infrared (IR) spectroscopy. The IR spectra of the gels of **1** obtained with or without sonication were almost the same, showing two peaks at $\nu = 1688$ and 1638 cm^{-1} corresponding to a hydrogen-bonded C=O vibration in the gel state.²⁵ This implies that C6=O plays a central role in the intermolecular hydrogen bonding of guanosine derivatives. Compared with the spectrum of **1**, sharp peaks appeared at $\nu = 1745$ and 1649 cm^{-1} in the infrared spectrum of **2**, evidencing that C6=O and branched ester groups did not participate in the intermolecular hydrogen-bonding interaction. This result was consistent with the morphological and structural studies (Fig. 7).

On the basis of the data presented above, the self-assembly processes of **1** and **2** can be clearly understood. Both the CD and NMR spectra support the formation of G-quartets consisting of two stacked G4 units with D_4 symmetry through multiple complementary N1-H...O6 and N2-H...O7 hydrogen bonds between the guanosine groups of **1** in acetonitrile in the concentration range 5.0×10^{-4} to 1.0×10^{-2} M (Fig. S7a, ESI[†]). It is remarkable that a derivative such as **1** can form G4-quartets in the absence of templating ions. We checked all of the experimental details and confirmed that no contaminant ions were present during the synthetic process. We noticed the formation of intermolecular interactions between amantadine groups, which may stabilize the stacking of G-quartets in dilute acetonitrile solution and also promote the formation

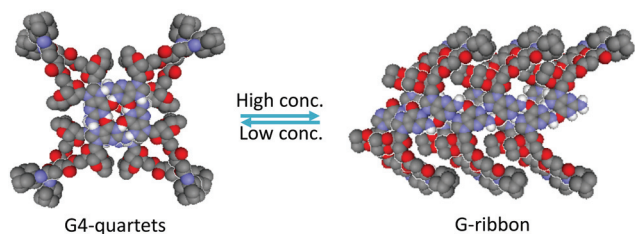


Fig. 8 The proposed structures of self-assembled G-quartets and G-ribbons by molecules of **1**.

and growth of G-ribbons with increasing concentration until the CGC is reached (Fig. 8). There are two kinds of G-ribbon structures, with the pairs of hydrogen bonds being N1–H...N7 and N2–H...O6 (type A) or N2–H...N7 and N1–H...O6 (type B), respectively (Fig. S7b and c, ESI[†]). Red-shifts of the CD and UV/visible absorption bands with increasing concentration indicated an increased dipole polarization in the aggregated state, which strongly supported the formation of a G-ribbon of type A. NMR spectra also indicated a decrease in the amount of the *anti*-rotamer of **1** in the formation of the G-ribbon. The most important finding was the tunable self-assembly of **1** by concentration and sonication, that is, the G-ribbon structure in the gel state could revert to G-quartets by dilution of the gel. In contrast, it was difficult to form ordered aggregates of **2** in a solvent due to its steric effect. This study has furthered our understanding of the formation, stability, and transformation of G-quartets.

Conclusions

We have designed and synthesized two guanosine derivatives by modification of this nucleobase with adamantane branches. The amphiphilic compound **1** with a single adamantane branch formed gels in acetonitrile and dichloromethane after a heating-cooling process, while compound **2** with three adamantane branches proved to be soluble in most polar solvents but precipitated from acetonitrile. By means of CD, UV, NMR, and IR spectroscopies, together with SEM and XRD, the influence of the structure and external conditions on the self-assembly behavior of the two compounds in acetonitrile has been extensively investigated. Compound **1** self-assembled into G-quartets in acetonitrile solution, which were transformed into a G-ribbon gel at concentrations higher than the CGC. The gel network was found to have a hexagonal columnar structure composed of G-ribbons, built from hydrogen-bonding and hydrophobic interactions. Moreover, the conversion between G-quartets and the G-ribbon structure could be reversibly controlled by varying the concentration. In contrast, due to the steric effect, multiple hydrogen bonding between the guanosine moieties in **2** was inhibited. As a result, **2** could only assemble into a spherical structure based on hydrophobic interactions. The use of designer bases to build discrete assemblies is clearly important in supramolecular chemistry and nanoscience.¹ The exploration of the conversion between

G-quartets and other self-assembled forms of guanosine has provided insight into the formation and stability of DNA G-quadruplexes. Moreover, it is evident that structural differences have a significant impact on the self-assembly mode in the construction of functional materials based on guanosine.

This work was supported by the China National Funds for Distinguished Young Scientists (21125104), National Natural Science Foundation of China (91022021), National Basic Research Program of China (2009CB930400, 2013CB733700), Program for Innovative Research Team in University (IRT1117), Program of Shanghai Subject Chief Scientist (12XD1405900), and Shanghai Leading Academic Discipline Project (B108).

Notes and references

- E. Krieg, H. Weissman, E. Shirman, E. Shimoni and B. Rybtchinski, *Nat. Nanotechnol.*, 2011, **6**, 141–146;
- J. T. Davis and G. P. Spada, *Chem. Soc. Rev.*, 2007, **36**, 296–313; A. R. Hirst, B. Escuder, J. F. Miravet and D. K. Smith, *Angew. Chem., Int. Ed.*, 2008, **47**, 8002–8018;
- R. Madueno, M. T. Raisanen, C. Silien and M. Buck, *Nature*, 2008, **454**, 618–621.
- J. L. Sessler and R. Z. Wang, *Angew. Chem., Int. Ed.*, 1998, **37**, 1726–1729.
- N. Sreenivasachary and J. M. Lehn, *Proc. Natl. Acad. Sci. U. S. A.*, 2005, **102**, 5938–5943; A. Wong and G. Wu, *J. Am. Chem. Soc.*, 2003, **125**, 13895–13905; D. Gonzalez-Rodriguez, P. G. A. Janssen, R. Martin-Rapun, I. De Cat, S. De Feyter, A. P. H. J. Schenning and E. W. Meijer, *J. Am. Chem. Soc.*, 2010, **132**, 4710–4719.
- G. Gottarelli, S. Masiero, E. Mezzina, S. Pieraccini, J. P. Rabe, P. Samori and G. P. Spada, *Chem.–Eur. J.*, 2000, **6**, 3242–3248; T. Giorgi, F. Grepioni, I. Manet, P. Mariani, S. Masiero, E. Mezzina, S. Pieraccini, L. Saturni, G. P. Spada and G. Gottarelli, *Chem.–Eur. J.*, 2002, **8**, 2143–2152.
- S. Lena, M. A. Cremonini, F. Federiconi, G. Gottarelli, C. Graziano, L. Laghi, P. Mariani, S. Masiero, S. Pieraccini and G. P. Spada, *Chem.–Eur. J.*, 2007, **13**, 3441–3449; G. Wu and I. C. M. Kwan, *J. Am. Chem. Soc.*, 2009, **131**, 3180–3182.
- S. Lena, S. Masiero, S. Pieraccini and G. P. Spada, *Chem.–Eur. J.*, 2009, **15**, 7792–7806; Y. F. Gao, Y. J. Huang, S. Y. Xu, W. J. Ouyang and Y. B. Jiang, *Langmuir*, 2011, **27**, 2958–2964; G. P. Spada, S. Lena, S. Masiero, S. Pieraccini, M. Surin and P. Samori, *Adv. Mater.*, 2008, **20**, 2433–2438; I. Yoshikawa, J. Li, Y. Sakata and K. Araki, *Angew. Chem., Int. Ed.*, 2004, **43**, 100–103.
- S. L. Forman, J. C. Fettinger, S. Pieraccini, G. Gottarelli and J. T. Davis, *J. Am. Chem. Soc.*, 2000, **122**, 4060–4067.
- M. Gellert, M. N. Lipsett and D. R. Davies, *Proc. Natl. Acad. Sci. U. S. A.*, 1962, **48**, 2013–2018.
- H. Y. Han and L. H. Hurley, *Trends Pharmacol. Sci.*, 2000, **21**, 136–142; K. A. Olausson, K. Dubrana, J. Dornont, J. P. Spano, L. Sabatier and J. C. Soria, *Crit. Rev. Oncol. Hematol.*, 2006, **57**, 191–214.

- 10 J. L. Sessler, M. Sathiosatham, K. Doerr, V. Lynch and K. A. Abboud, *Angew. Chem., Int. Ed.*, 2000, **39**, 1300–1303.
- 11 R. Otero, M. Schock, L. M. Molina, E. Laegsgaard, I. Stensgaard, B. Hammer and F. Besenbacher, *Angew. Chem., Int. Ed.*, 2005, **44**, 2270–2275.
- 12 A. Ciesielski, S. Lena, S. Masiero, G. P. Spada and P. Samori, *Angew. Chem., Int. Ed.*, 2010, **49**, 1963–1966; X. G. Wang, L. P. Zhou, H. Y. Wang, Q. A. Luo, J. Y. Xu and J. Q. Liu, *J. Colloid Interface Sci.*, 2011, **353**, 412–419.
- 13 E. M. Rezler, D. J. Bearss and L. H. Hurley, *Annu. Rev. Pharmacol.*, 2003, **43**, 359–379; D. Koirala, S. Dhakal, B. Ashbridge, Y. Sannohe, R. Rodriguez, H. Sugiyama, S. Balasubramanian and H. B. Mao, *Nat. Chem.*, 2011, **3**, 782–787; T. Mashimo, H. Yagi, Y. Sannohe, A. Rajendran and H. Sugiyama, *J. Am. Chem. Soc.*, 2010, **132**, 14910–14918.
- 14 C. Wang, Z. Q. Wang and X. Zhang, *Acc. Chem. Res.*, 2012, **45**, 608–618.
- 15 J. Sawayama, H. Sakaino, S. Kabashima, I. Yoshikawa and K. Araki, *Langmuir*, 2011, **27**, 8653–8658; S. Lena, S. Masiero, S. Pieraccini and G. P. Spada, *Mini-Rev. Org. Chem.*, 2008, **5**, 262–273; R. N. Das, Y. P. Kumar, S. Pagoti, A. J. Patil and J. Dash, *Chem.–Eur. J.*, 2012, **18**, 6008–6014.
- 16 P. Terech and R. G. Weiss, *Chem. Rev.*, 1997, **97**, 3133–3159; J. H. Jung, M. Park and S. Shinkai, *Chem. Soc. Rev.*, 2010, **39**, 4286–4302; A. Vintiloiu and J. C. Leroux, *J. Controlled Release*, 2008, **125**, 179–192; D. Hu, J. S. Ren and X. G. Qu, *Chem. Sci.*, 2011, **2**, 1356–1361; W. J. Wang, Q. H. Chen, Q. Li, Y. Sheng, X. J. Zhang and K. Uvdal, *Cryst. Growth Des.*, 2012, **12**, 2707–2713; X. Zhang, X. Chu, L. Wang, H. Wang, G. Liang, J. Zhang, J. Long and Z. Yang, *Angew. Chem., Int. Ed.*, 2012, **51**, 4388–4392; N. M. Sangeetha and U. Maitra, *Chem. Soc. Rev.*, 2005, **34**, 821–836; J. Wu, T. Yi, T. Shu, M. Yu, Z. Zhou, M. Xu, Y. Zhou, H. Zhang, J. Han, F. Li and C. Huang, *Angew. Chem., Int. Ed.*, 2008, **47**, 1063–1067; X. Yu, Q. Liu, J. Wu, M. Zhang, X. Cao, S. Zhang, Q. Wang, L. Chen and T. Yi, *Chem.–Eur. J.*, 2010, **16**, 9099–9106; M. Zhang, L. Meng, X. Cao, M. Jiang and T. Yi, *Soft Matter*, 2012, **8**, 4494–4498.
- 17 B. L. Zhang, Z. Y. Cui and L. L. Sun, *Org. Lett.*, 2001, **3**, 275–278; S. Capel-Cuevas, I. de Orbe-Paya, F. Santoyo-Gonzalez and L. F. Capitan-Vallvey, *Talanta*, 2009, **78**, 1484–1488.
- 18 R. K. O. Sigel and H. Sigel, *Acc. Chem. Res.*, 2010, **43**, 974–984.
- 19 D. Gonzalez-Rodriguez, J. L. J. van Dongen, M. Lutz, A. L. Spek, A. P. H. J. Schenning and E. W. Meijer, *Nat. Chem.*, 2009, **1**, 151–155.
- 20 G. Gottarelli, S. Lena, S. Masiero, S. Pieraccini and G. P. Spada, *Chirality*, 2008, **20**, 471–485.
- 21 S. Masiero, R. Trotta, S. Pieraccini, S. De Tito, R. Perone, A. Randazzo and G. P. Spada, *Org. Biomol. Chem.*, 2010, **8**, 2683–2692.
- 22 M. Panda and J. A. Walmsley, *J. Phys. Chem. B*, 2011, **115**, 6377–6383.
- 23 G. Gottarelli, S. Masiero and G. P. Spada, *J. Chem. Soc., Chem. Comm.*, 1995, 2555–2557; A. L. Marlow, E. Mezzina, G. P. Spada, S. Masiero, J. T. Davis and G. Gottarelli, *J. Org. Chem.*, 1999, **64**, 5116–5123.
- 24 S. Pieraccini, S. Bonacchi, S. Lena, S. Masiero, M. Montalti, N. Zaccheroni and G. P. Spada, *Org. Biomol. Chem.*, 2010, **8**, 774–781; E. Mezzina, P. Mariani, R. Itri, S. Masiero, S. Pieraccini, G. P. Spada, F. Spinozzi, J. T. Davis and G. Gottarelli, *Chem.–Eur. J.*, 2001, **7**, 388–395.
- 25 I. Yoshikawa, S. Yanagi, Y. Yamaji and K. Araki, *Tetrahedron*, 2007, **63**, 7474–7481.